2005 International Linear Collider Workshop - Stanford, U.S.A.

Neutrinos in Supersymmetry

Marco Aurelio Díaz
Department of Physics, Universidad Católica de Chile, Santiago, Chile

We briefly review the neutrino mass generation mechanism in supersymmetry with Bilinear R-Parity Violation in Minimal Supergravity and Anomaly Mediated Supersymmetry Breaking.

1. INTRODUCTION

Experimental results indicate that neutrinos oscillate: the three known neutrino flavour states ν_e, ν_μ, and ν_τ, are linear combinations of the mass eigenstates ν_1, ν_2, and ν_3, inducing neutrino oscillations in vacuum [1] and in matter [2]. The experimental results come from many experiments such as, Kamiokande, SAGE, GALLEX, GNO, Super-Kamiokande, and SNO for solar neutrino [3]; KamLAND for long-baseline reactor neutrino [4]; Kamiokande, Super-Kamiokande, MACRO, and Soudan-2 for atmospheric neutrino [5]; K2K for long-baseline accelerator neutrino [6]; and CHOOZ and Palo Verde for short-baseline accelerator neutrino experiments [7].

The neutrino mass matrix is diagonalized with the matrix [8]

$$U_{PMNS} = \begin{pmatrix} 1 & 0 & 0 \\ 0 & \cos\theta_{23} & \sin\theta_{23} \\ 0 & -\sin\theta_{23} & \cos\theta_{23} \end{pmatrix} \begin{pmatrix} \cos\theta_{13} & 0 & \sin\theta_{13} \\ 0 & 1 & 0 \\ -\sin\theta_{13} & 0 & \cos\theta_{13} \end{pmatrix} \begin{pmatrix} \cos\theta_{23} & \sin\theta_{23} & 0 \\ -\sin\theta_{23} & \cos\theta_{23} & 0 \\ 0 & 0 & 1 \end{pmatrix} \tag{1}$$

This matrix may contain also a Dirac and two Majorana phases [9], which we assume to be absent. The oscillations are defined by the atmospheric θ_{23}, solar θ_{12} and reactor θ_{13} mixing angles, and the atmospheric Δm^2_{32} and solar Δm^2_{21} mass squared differences.

There are several analysis of these experimental results [10]. We use the 3σ allowed regions for the neutrino parameters in [11], given by

$$\begin{aligned} 1.4\times10^{-3} < \Delta m^2_{32} < 3.3\times10^{-3}\,\mathrm{eV}^2 \qquad & 0.52 < \tan^2\theta_{23} < 2.1 \\ 7.2\times10^{-5} < \Delta m^2_{21} < 9.1\times10^{-5}\,\mathrm{eV}^2 \qquad & 0.30 < \tan^2\theta_{12} < 0.61 \end{aligned} \tag{2}$$

which we complete with the upper bound $\tan^2\theta_{13} < 0.049$ for the reactor angle.

2. LOW ENERGY SEESAW MECHANISM

We study here the generation of neutrino masses in supersymmetry with Bilinear R-Parity Violation (BRpV). The superpotential of our model differs from the MSSM by three terms which violate R-Parity and lepton number [12],

$$W = W_{MSSM} + \epsilon_i \hat{L}_i \hat{H}_u \tag{3}$$

where ϵ_i have units of mass. These bilinear terms induce mixing between the neutralinos and neutrinos, forming a 7×7 mass matrix. A low energy seesaw mechanism induces the following effective 3×3 neutrino mass matrix

$$\mathbf{M}^{(0)}_\nu = \frac{M_1 g^2 + M_2 g'^2}{4\,det(\mathcal{M}_{\chi^0})} \begin{bmatrix} \Lambda_1^2 & \Lambda_1\Lambda_2 & \Lambda_1\Lambda_3 \\ \Lambda_1\Lambda_2 & \Lambda_2^2 & \Lambda_2\Lambda_3 \\ \Lambda_1\Lambda_3 & \Lambda_2\Lambda_3 & \Lambda_3^2 \end{bmatrix} \tag{4}$$

where we have defined the parameters $\Lambda_i = \mu v_i + \epsilon_i v_d$, which are proportional to the sneutrino vacuum expectation values in the basis where the ϵ terms are removed from the superpotential. At tree-level only one neutrino acquire a mass, and one-loop corrections must be included [13].

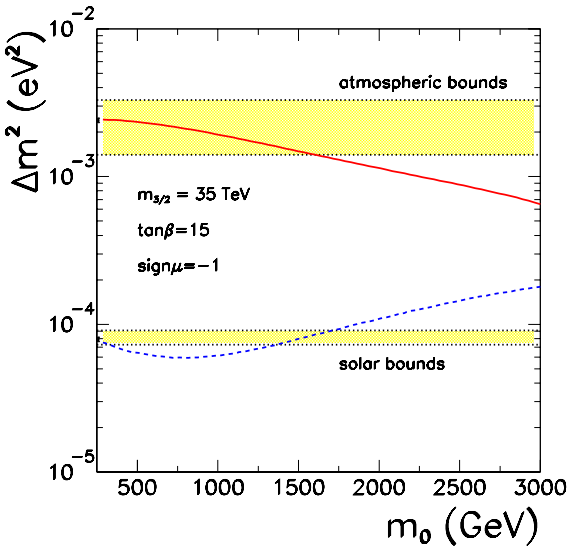

Figure 1: The red solid (blue hashed) line stands for the predicted atmospheric (solar) mass squared difference as a function of the scalar mass m_0 for $m_{3/2} = 35$ TeV, $\tan\beta = 15$, and $\text{sign}(\mu) < 0$ and for the BRpV parameters given in (6). The allowed 3σ atmospheric (solar) mass squared difference is represented by the upper (lower) horizontal yellow band. Our reference point is represented by a star on the left of the plot.

3. ANOMALY MEDIATED SUSY BREAKING

In AMSB-BRpV we work with [14, 15]

$$m_{3/2} = 35\,\text{TeV}\,, \quad m_0 = 250\,\text{GeV}\,, \quad \tan\beta = 15\,, \quad \text{and} \quad \text{sign}(\mu) < 0\,. \tag{5}$$

and we randomly vary the parameters ϵ_i and Λ_i looking for solutions in which the restrictions (2) from neutrino physics are satisfied. An example of these solutions is

$$\begin{aligned} &\epsilon_1 = -0.015\ \text{GeV}\,, \qquad \epsilon_2 = -0.018\ \text{GeV}\,, \qquad \epsilon_3 = 0.011\ \text{GeV}\,, \\ &\Lambda_1 = -0.03\ \text{GeV}^2\,, \qquad \Lambda_2 = -0.09\ \text{GeV}^2\,, \qquad \Lambda_3 = -0.09\ \text{GeV}^2\,. \end{aligned} \tag{6}$$

The neutrino parameters obtained in this reference model are

$$\begin{aligned} &\Delta m^2_{\text{atm}} = 2.4\times10^{-3}\,\text{eV}^2\,, \qquad \tan^2\theta_{\text{atm}} = 0.72\,, \qquad \tan^2\theta_{13} = 0.033\,, \\ &\Delta m^2_{\text{sol}} = 7.9\times10^{-5}\,\text{eV}^2\,, \qquad \tan^2\theta_{\text{sol}} = 0.47\,, \end{aligned} \tag{7}$$

which agree with the present experimental results. The neutrino mass matrix has the following texture

$$\mathbf{M}_\nu^{eff} = m\begin{bmatrix} \lambda & 2\lambda & \lambda \\ 2\lambda & a & b \\ \lambda & b & 1 \end{bmatrix} \tag{8}$$

with $a \sim 0.74$, $b \sim 0.67$, $\lambda \sim 0.13$, and $m \sim 0.032$ eV.

In Fig. 1 it is shown the dependence on the scalar mass m_0 of the predicted atmospheric neutrino mass squared difference Δm^2_{atm} (red solid line) and the solar neutrino mass squared difference Δm^2_{sol} (blue dashed line), for fixed values $m_{3/2} = 35$ TeV, $\tan\beta = 15$, and $\text{sign}(\mu) < 0$ and for the BRpV parameters given in (6). We see from Fig. 1 that Δm^2_{atm} is within the present experimental bounds for $m_0 \lesssim 1.6$ TeV while Δm^2_{sol} satisfies the experimental constraints for $m_0 \lesssim 310$ GeV and 1.4 TeV $\lesssim m_0 \lesssim 1.75$ TeV. Therefore, our models lead to acceptable neutrino

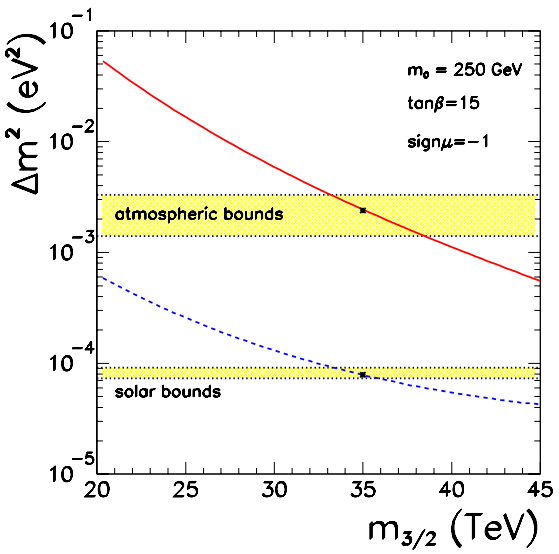

Figure 2: Atmospheric (solid line) and solar (dashed line) mass squared differences as a function of the gravitino mass $m_{3/2}$. The remaining parameters assume the value of our reference point and the conventions are the same of Fig. 1.

masses provided $m_0 \lesssim 310$ GeV or 1.4 TeV $\lesssim m_0 \lesssim 1.6$ TeV for all other parameters fixed at their reference values. It is also important to notice that the heaviest neutrino state has a mass of the order of 0.050 eV for our reference point and that it decreases as m_0 increases. Moreover, the radiative corrections lead to a contribution of $\mathcal{O}(10\%)$, therefore, the tree–level result for the neutrino mass is a good order of magnitude estimative.

In Fig. 2 we display the dependence of the atmospheric and solar mass squared differences on the gravitino mass $m_{3/2}$ for the other parameters assuming their reference values. First of all, the observed dependence is much stronger compared to the dependence on m_0; this is expected due to the large impact of $m_{3/2}$ on the soft gaugino masses, which together with μ define the tree–level neutrino mass matrix. Moreover, the SUSY spectrum has a large impact on the one–loop corrections increasing the sensitivity to $m_{3/2}$. Both solar and atmospheric squared mass differences are too large in the region of small gravitino masses, however, this region is already partially ruled out since it leads to charginos lighter than the present experimental bounds for $m_{3/2} \lesssim 30$ TeV. Conversely, there is no acceptable solution for the neutrino masses at large $m_{3/2}$, again a region partially ruled out by data since the staus are too light in this region. Furthermore, we can see from this figure that our AMSB–BRpV model leads to acceptable neutrino masses for a small window of the gravitino mass (33 TeV $\lesssim$ m$_{3/2} \lesssim$ 36 TeV) given our choice of parameters. This is far from trivial since we have no *a priori* guaranty that we can generate the required neutrino spectrum, specially the radiative corrections, satisfying at the same time the experimental constraints on the superpartner masses.

4. MINIMAL SUPERGRAVITY

Our analysis in Sugra-BRpV is defined by [16]

$$m_0 = 100\,\text{GeV}\,,\; M_{1/2} = 250\,\text{GeV}\,,\; A_0 = -100\,\text{GeV}\,,\; \tan\beta = 10\,,\; \mu > 0 \tag{9}$$

where the neutralino is the LSP with a mass $m_{\chi_1^0} = 99$ GeV, and the light neutral Higgs boson with $m_h = 114$ GeV.

In this context we find several solutions for neutrino physics which satisfy the experimental constraints on the atmospheric and solar mass squared differences, and the three mixing angles. We single out the following

$$\begin{aligned} \epsilon_1 &= -0.0004\,, & \epsilon_2 &= 0.052\,, & \epsilon_3 &= 0.051\,, \\ \Lambda_1 &= 0.022\,, & \Lambda_2 &= 0.0003\,, & \Lambda_3 &= 0.039\,, \end{aligned} \tag{10}$$

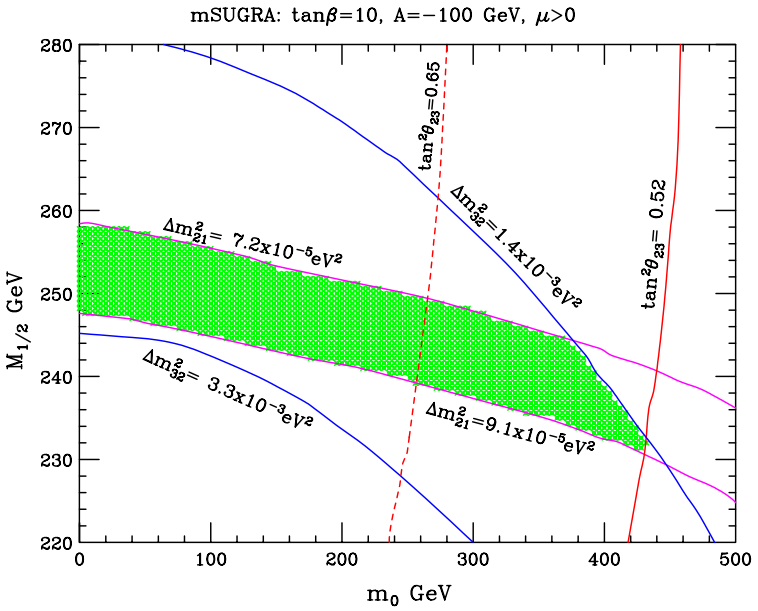

Figure 3: Region of parameter space in the plane $m_0 - M_{1/2}$ where solutions to neutrino physics passing all the implemented experimental cuts are located. Contours of constant atmospheric mass difference and angle, and solar mass difference are displayed.

This solution is characterized by

$$\begin{aligned} \Delta m^2_{\rm atm} &= 2.7\times 10^{-3}\,{\rm eV}^2\,, \qquad \tan^2\theta_{\rm atm} = 0.72\,, \qquad \tan^2\theta_{13} = 0.0058\,, \\ \Delta m^2_{\rm sol} &= 8.1\times 10^{-5}\,{\rm eV}^2\,, \qquad \tan^2\theta_{\rm sol} = 0.54\,, \end{aligned} \tag{11}$$

which are well inside the experimentally allowed window in eq. (2). We note that the random solution in eq. (10) is compatible with $\epsilon_1 = \Lambda_2 = 0$, *i.e.*, the neutrino parameters in eq. (11) are hardly changed with this replacement. The neutrino mass matrix has the following texture

$$\mathbf{M}_\nu^{eff} = m \begin{bmatrix} \lambda & 0 & \lambda \\ 0 & a & a \\ \lambda & a & 1 \end{bmatrix} \tag{12}$$

with $a \sim 0.75$, $\lambda \sim 0.14$, and $m \sim 0.033$ eV.

In Fig. 3 we take the neutrino solution given by the BRpV parameters in eq. (10), and vary the scalar mass m_0 and the gaugino mass $M_{1/2}$, looking for solutions that satisfy all experimental cuts. In this case, sugra points satisfying the experimental restrictions on the neutrino parameters lie in the shaded region. Solutions are concentrated in a narrow band defined by $M_{1/2} \approx 230 - 260$ GeV and $m_0 \approx 0 - 400$ GeV. We note that in BRpV the LSP need not to be the lightest neutralino, since it is not stable anyway. For this reason, the region close to $m_0 \approx 0$ is not ruled out.

Smaller values of $M_{1/2}$ are not possible because the atmospheric and solar mass differences become too large. The allowed strip is, thus, limited from below by the curve $\Delta m^2_{21} = 9.1\times 10^{-5}$ eV^2. The dependency on $M_{1/2}$ is felt stronger by the tree level contribution. Higher values of the scalar mass m_0 are not allowed because the atmospheric angle becomes too small. The allowed strip is, therefore, limited from the right by the contour $\tan^2\theta_{23} = 0.52$. High values of the scalar mass are also limited from above because the atmospheric mass becomes too large. Higher values of $M_{1/2}$ are not possible because the solar mass becomes too small, therefore, the allowed stripe is limited from above by the line $\Delta m^2_{21} = 7.2\times 10^{-5}$ eV^2.

In Fig. 4 we plot the inverse of the partial decay width (multiplied by the velocity of light to convert it into a distance) as a function of the most relevant BRpV parameters. In frame (4a) we see the inverse of $\Gamma(\chi^0_1 \to We)$ as a function of Λ_1. In fact, for all practical purposes, the decay rate into electrons depends *only* on Λ_1. Since in first

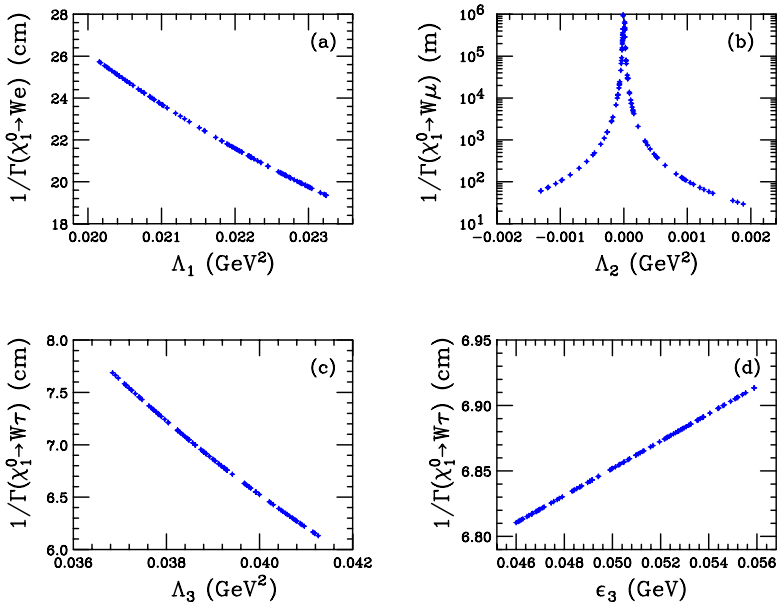

Figure 4: Partial decay width of a neutralino into a W and a lepton, measured in units of distance.

approximation, the coupling is proportional to Λ_1, the inverse of the decay rate behaves like Λ_1^{-2}, and this is seen in the figure. The values of Λ_1 are limited by the solar parameters. The inverse of the partial decay rate $\chi_1^0 \to We$ is of the order of $20 - 25\,cm$, and it's an important part of the total decay rate.

In frame (4b) we have the inverse of $\Gamma(\chi_1^0 \to W\mu)$ as a function of Λ_2, and similarly to the previous case, the decay rate into muons depends practically only on Λ_2. In our reference model in eq. (10) we have $\Lambda_2 \approx 0$, but values indicated in the figure are also compatible with neutrino physics. The coupling of the neutralino to W and muon is proportional to Λ_2, so the inverse of the decay rate goes like Λ_2^{-2}, and that is observed in frame (4b). Depending on the value of Λ_2, the partial decay length vary from centimeters to kilometers in the figure. Therefore, this partial decay rate contribute little to the total decay rate of the neutralino.

The inverse of $\Gamma(\chi_1^0 \to W\tau)$ is plotted in frames (4c) and (4d) as a function of Λ_3 and ϵ_3 respectively. The dependence on Λ_3 is stronger and similarly to the previous cases it goes like Λ_3^{-2}. The dependence on ϵ_3 is weaker, and the inverse decay rate increases with this parameter. The inverse decay rate is of the order of $7\,cm$, making it the most important contribution to the total decay rate. Including the decay modes into neutrinos and a Z, the total inverse decay rate is near $4\,cm$. The ratios of branching ratios for our benchmark point in eq. (10) are given by

$$\frac{B(\chi_1^0 \to W\mu)}{B(\chi_1^0 \to W\tau)} = 5.9 \times 10^{-5}\,, \qquad \frac{B(\chi_1^0 \to We)}{B(\chi_1^0 \to W\tau)} = 0.32 \tag{13}$$

We note that if we increase Λ_2 by a factor 4, the first ratio of branching ratios increase to $\sim 10^{-3}$ without changing the other ratio, while still passing all the experimental cuts. From this figure, it is clear that by measuring the branching ratios of the neutralinos we get information on the parameters of the model.

We calculate the production cross sections $\sigma(pp \to \chi_1^0\chi_1^0)$ (LHC) and $\sigma(e^+e^- \to \chi_1^0\chi_1^0)$ (ILC at $\sqrt{s} = 500$ GeV) at leading order, and using the branching ratios find

$$\begin{aligned} \sigma(pp \to \chi_1^0\chi_1^0 \to W^+W^+e^-\tau^-) &= 3.4 \times 10^{-4}\ \text{pb} \\ \sigma(e^+e^- \to \chi_1^0\chi_1^0 \to W^+W^+e^-\tau^-) &= 9.3 \times 10^{-3}\ \text{pb} \end{aligned} \tag{14}$$

with negligible background. Assuming a luminosity of 10^5 pb^{-1}/year at both machines, we expect ~ 280 signal event per year at the LHC and ~ 3700 signal events per year at the ILC (summing over lepton charges).

5. CONCLUSIONS

Supersymmetry with Bilinear R-Parity Violation remains a viable mechanism for the generation of neutrino masses and mixing angles. In this model, the neutralino is no longer a candidate to dark matter. Nevertheless, it is possible to understand the neutrino mass spectrum. A low energy seesaw mechanism gives mass to one neutrino due to the mixing with neutralinos, and quantum corrections give mass to the other two. We show examples on how this works in supergravity and AMSB, indicating how this model can be tested in future colliders.

Acknowledgments

This research was partly founded by CONICYT grant No. 1040384.

References

[1] B. Pontecorvo, *Zh. Eksp. Teor. Fiz. 53*, 1717 (1968) [*Sov. Phys. JETP* **26**, 984 (1968)]; Z. Maki, M. Nakagawa, S. Sakata, *Prog. Theor. Phys.* **28**, 870 (1962).

[2] L. Wolfenstein, *Phys. rev. D* **17**, 2369 (1978); S.P. Mikheev, A. Yu. Smirnov, *Yad. Fiz.* **42**, 1441 (1985) [*Sov. J. Nucl. Phys.* **42**, 913 (1985)].

[3] Y. Fukuda *et al.* [Kamiokande Collaboration], Phys. Rev. Lett. **77** (1996) 1683; J. N. Abdurashitov *et al.* [SAGE Collaboration], J. Exp. Theor. Phys. **95** (2002) 181 [Zh. Eksp. Teor. Fiz. **122** (2002) 211]; W. Hampel *et al.* [GALLEX Collaboration], Phys. Lett. B **447** (1999) 127; M. Altmann *et al.* [GNO COLLABORATION Collaboration], Phys. Lett. B **616** (2005) 174; S. Fukuda *et al.* [Super-Kamiokande Collaboration], Phys. Lett. B **539** (2002) 179; Q. R. Ahmad *et al.* [SNO Collaboration], Phys. Rev. Lett. **89** (2002) 011301.

[4] K. Eguchi *et al.* [KamLAND Collaboration], Phys. Rev. Lett. **90** (2003) 021802.

[5] S. Hatakeyama *et al.* [Kamiokande Collaboration], Phys. Rev. Lett. **81** (1998) 2016; Y. Fukuda *et al.* [Super-Kamiokande Collaboration], Phys. Rev. Lett. **81** (1998) 1562; M. Ambrosio *et al.* [MACRO Collaboration], Eur. Phys. J. C **36** (2004) 323; M. C. Sanchez *et al.* [Soudan 2 Collaboration], Phys. Rev. D **68** (2003) 113004.

[6] M. H. Ahn *et al.* [K2K Collaboration], Phys. Rev. Lett. **90** (2003) 041801.

[7] M. Apollonio *et al.* [CHOOZ Collaboration], Phys. Lett. B **466** (1999) 415; F. Boehm *et al.*, Phys. Rev. D **64** (2001) 112001.

[8] G. L. Fogli, E. Lisi, A. Marrone and A. Palazzo, arXiv:hep-ph/0506083.

[9] J. Schechter and J. W. F. Valle, Phys. Rev. D **22** (1980) 2227.

[10] H. Nunokawa, W. J. C. Teves and R. Zukanovich Funchal, Phys. Lett. B **562** (2003) 28; P. C. de Holanda and A. Y. Smirnov, JCAP **0302** (2003) 001; P. Aliani, V. Antonelli, M. Picariello and E. Torrente-Lujan, Phys. Rev. D **69** (2004) 013005; J. N. Bahcall, M. C. Gonzalez-Garcia and C. Pena-Garay, JHEP **0302** (2003) 009; G. L. Fogli, E. Lisi, A. Marrone, D. Montanino, A. Palazzo and A. M. Rotunno, Phys. Rev. D **67** (2003) 073002; V. Barger and D. Marfatia, Phys. Lett. B **555** (2003) 144; A. Bandyopadhyay, S. Choubey, R. Gandhi, S. Goswami and D. P. Roy, Phys. Lett. B **559** (2003) 121.

[11] M. Maltoni, T. Schwetz, M. A. Tortola and J. W. F. Valle, arXiv:hep-ph/0405172.

[12] M. A. Diaz, J. C. Romao and J. W. F. Valle, Nucl. Phys. B **524** (1998) 23.

[13] J. C. Romao *et.al.*, Phys. Rev. D **61** (2000) 071703; M. Hirsch *et.al.*, Phys. Rev. D **62** (2000) 113008 [Erratum-ibid. D **65** (2002) 119901]; M. A. Diaz, M. Hirsch, W. Porod, J. C. Romao and J. W. F. Valle, Phys. Rev. D **68** (2003) 013009 [Erratum-ibid. D **71** (2005) 059904].

[14] F. de Campos *et.al.*, Phys. Rev. D **71** (2005) 055008.

[15] M. A. Diaz, R. A. Lineros and M. A. Rivera, Phys. Rev. D **67** (2003) 115004; F. De Campos, M. A. Diaz, O. J. P. Eboli, M. B. Magro and P. G. Mercadante, Nucl. Phys. B **623** (2002) 47

[16] M. A. Diaz, C. Mora and A. R. Zerwekh, arXiv:hep-ph/0410285.